Nonlinear Dyn (2012) 67:1525–1537
DOI 10.1007/s11071-011-0086-3

ORIGINAL PAPER

Robust control of flexible-joint robots using voltage control strategy

Mohammad Mehdi Fateh

Received: 20 May 2010 / Accepted: 12 May 2011 / Published online: 11 June 2011

Abstract So far, control of robot manipulators has frequently been developed based on the torque-control strategy. However, two drawbacks may occur. First, torque-control laws are inherently involved in complexity of the manipulator dynamics characterized by nonlinearity, largeness of model, coupling, uncertainty and joint flexibility. Second, actuator dynamics may be excluded from the controller design. The novelty of this paper is the use of voltage control strategy to develop robust tracking control of electrically driven flexible-joint robot manipulators. In addition, a novel method of uncertainty estimation is introduced to obtain the control law. The proposed control approach has important advantages over the torque-control approaches due to being free of manipulator dynamics. It is computationally simple, decoupled, well-behaved and has a fast response. The control design includes two interior loops; the inner loop controls the motor position and the outer loop controls the joint position. Stability analysis is presented and performance of the control system is evaluated. Effectiveness of the proposed control approach is demonstrated by simulations using a three-joint articulated flexible-joint robot driven by permanent magnet dc motors.

M.M. Fateh (✉)
Department of Electrical and Robotic Engineering, Shahrood University of Technology, Shahrood 3619995161, Iran
e-mail: mmfateh@shahroodut.ac.ir

Keywords Electrically driven flexible-joint robot · Robust control · Stability analysis · Voltage control strategy

1 Introduction

Electric motors provide low torque at high speed. They are equipped with power transmission systems to provide high torque at low speed for driving a robot. However, deformation of the transmission system produces flexibility in the joints. This phenomenon is the main source of vibration in industrial robot manipulators [1]. Compared with rigid robots, number of degrees of freedom becomes twice as number of control actions due to flexibility in the joints, and the matching property between nonlinearities and inputs is lost [2]. Performing high-precision applications by a flexible-joint robot seems to be difficult since the link position cannot directly follow the actuator position. As a result, the flexibility in joints should be compensated to improve the performance and avoid unwanted oscillations.

The flexible-joint robot manipulator presents serious problems such as nonlinearity, largeness of model, coupling, uncertainty, and joint flexibility in the modeling and control. This has attracted a great deal of research in developing advance controls. For instance, PD control [3], feedback linearization technique [4], integral manifold approach [5], singular perturbation theory [6], robust control [7], sliding mode control

[8], adaptive control [9], fuzzy control [10], learning control [11], neural network approach [12], passivity-based impedance control [13], state observer based control [14] have been devoted to deal with the control of flexible-joint robot. Time delay control [15] and uncertainty estimation [16] can be used to control such a complicated nonlinear system by estimating current effects of unknown dynamics and disturbances.

So far, robot manipulators have been frequently controlled using the torque-control strategy. However, two drawbacks may occur. First, the torque-control laws are inherently involved in complexity of the manipulator dynamics characterized by nonlinearity, largeness of model, coupling, uncertainty, and joint flexibility. Second, actuator dynamics may be excluded from the controller design. The novelty of this paper is the use of voltage control strategy for being free of manipulator dynamics. As a result, the proposed control approach is free of many effects caused by manipulator dynamics. This is an important advantage of the proposed control approach over the torque-based control approaches.

Based on the modeling analysis, four variables for each joint either "the position, velocity, acceleration and jerk of the link [7]" or "the position and velocity of the actuator and the link" are required to perform the feedback control [17]. Measuring the acceleration and jerk experiences many difficulties in practice. However, an observer may be used to substitute the actual variable. Assuming global link coordinates and their time derivatives as outputs, a nonlinear observer was proposed which asymptotically reconstructs all state variables [18]. However, an observer is designed based on the model, thus errors may be produced due to using an imprecise model. This paper develops a control approach that uses available feedbacks as an important advantage from practical point of view. The design includes two interior loops; the inner loop controls the motor position using the motor position and velocity while the outer loop controls the joint position by a PID (Proportional-Integral-Derivative) controller.

Feedback linearization is a helpful technique to facilitate the control design particularly by canceling the nonlinearities and decoupling the system. Generally, a flexible-joint robot cannot be feedback linearized by static feedback [3]. However, under some assumptions, a simplified model was introduced which can be feedback linearized [7]. Moreover, it was proven that the whole class of elastic joint robots could be linearized via dynamic feedback [19]. However, model of the flexible robot is so large, computationally extensive and imprecise. Thus, model-based techniques such as feedback linearization cannot work well. This paper proposes a control law that is free of manipulator dynamics.

To overcome uncertainty, many valuable robust control approaches have been developed to control robot manipulators in the joint-space [20, 21] and in the task-space [22, 23]. However, robust control may involve in complexity raised from the manipulator dynamics. Great attention has been attracted to overcoming this shortcoming. A proper uncertainty bound parameter has been proposed to simplify and improve robust control of robot manipulators [24]. It is found that the voltage control strategy [25] is superior to the torque-control strategy in the robust control of rigid manipulators [26] in terms of simplicity in the controller design and performance of the control system. Since flexibility in the joints provides a complex dynamics, the voltage control strategy will be more efficient than the torque-control strategy. This paper uses the voltage control strategy for robust tracking control of electrically driven flexible-joint robot manipulators. In addition, a novel method of uncertainty estimation is introduced and used to obtain the control law. Stability analysis is presented and effectiveness of the proposed control approach is demonstrated by simulations.

This paper is organized as follows: Section 2 develops modeling of the electrical flexible-joint manipulator driven by geared permanent magnet dc motors. Section 3 presents the proposed robust control. Section 4 deals with stability analysis and performance evaluation. Section 6 considers the uncertainty estimation. Section 7 presents the simulation results and finally, Section 7 concludes the paper.

2 Modeling

In a simplified model of flexible-joint robot [7], the manipulator links are assumed rigid and motors are elastically coupled to the links. The motor torques are assumed as inputs of the robotic system. In this paper, the simplified model is applied for an electrically driven robot with some modifications to obtain the motor voltages as the inputs. Consider a robot with revolute joints driven by geared permanent magnet dc motors. If the joint flexibility is modeled by a linear tor-

sional spring, dynamic equation of motion can be expressed as

$$\mathbf{D}(\boldsymbol{\theta})\ddot{\boldsymbol{\theta}} + \mathbf{C}(\boldsymbol{\theta}, \dot{\boldsymbol{\theta}})\dot{\boldsymbol{\theta}} + \mathbf{g}(\boldsymbol{\theta}) = \mathbf{K}(\mathbf{r}\boldsymbol{\theta}_m - \boldsymbol{\theta}) \tag{1}$$

$$\mathbf{J}\ddot{\boldsymbol{\theta}}_m + \mathbf{B}\dot{\boldsymbol{\theta}}_m + \mathbf{r}\mathbf{K}(\mathbf{r}\boldsymbol{\theta}_m - \boldsymbol{\theta}) = \boldsymbol{\tau} \tag{2}$$

where $\boldsymbol{\theta} \in R^n$ is a vector of joint angles and $\boldsymbol{\theta}_m \in R^n$ is a vector of rotor angles. Thus, this system possesses $2n$ coordinates as $[\,\boldsymbol{\theta}\ \boldsymbol{\theta}_m\,]$. $\mathbf{D}(\boldsymbol{\theta})$ is a $n \times n$ matrix of manipulator inertia, $\mathbf{C}(\boldsymbol{\theta}, \dot{\boldsymbol{\theta}})\ \dot{\boldsymbol{\theta}} \in R^n$ is a vector of centrifugal and Coriolis forces, $\mathbf{g}(\boldsymbol{\theta}) \in R^n$ is a vector of gravitational forces and $\boldsymbol{\tau} \in R^n$ is a torque vector of motors. $\mathbf{J}$, $\mathbf{B}$ and $\mathbf{r}$ are $n \times n$ diagonal matrices to represent coefficients of the motor inertia, motor damping and reduction gear, respectively. The diagonal matrix $\mathbf{K}$ represents the lumped flexibility provided by the joint and reduction gear. To simplify the model, both the joint stiffness and gear coefficients are assumed constant. The vector of gravitational forces $\mathbf{g}(\boldsymbol{\theta})$ is assumed function of only the joint positions as used in the simplified model [7]. Note that vectors and matrices are represented in bold form for clarity.

System (1)–(2) is highly nonlinear, extensively computational, heavily coupled, multi-input/multi-output system with the $2n$ coordinates. Complexity of the model has been a serious challenge in robot modeling and control in literature. It is expected to face a higher complexity if the proposed model includes the actuator dynamics. In order to obtain the motor voltages as inputs, consider electrical equation of the geared permanent magnet dc motors in the matrix form

$$\mathbf{v} = \mathbf{R}\mathbf{I}_a + \mathbf{L}\dot{\mathbf{I}}_a + \mathbf{K}_b\dot{\boldsymbol{\theta}}_m \tag{3}$$

where $\mathbf{v} \in R^n$ is a vector of motor voltages, $\mathbf{I}_a \in R^n$ is a vector of motor currents and $\dot{\boldsymbol{\theta}}_m$ is a vector of rotor velocities. $\mathbf{R}$, $\mathbf{L}$ and $\mathbf{K}_b$ represent the $n \times n$ diagonal matrices for the coefficients of armature resistance, armature inductance, and back-emf constant, respectively. The motor torques $\boldsymbol{\tau}$ as input for dynamic equation (2) is produced by the motor currents as

$$\mathbf{K}_m\mathbf{I}_a = \boldsymbol{\tau} \tag{4}$$

where $\mathbf{K}_m$ is a diagonal matrix of the torque constants. Equations (1)–(4) form the robotic system such that the voltage vector $\mathbf{v}$ is the input vector and the joint angle vector $\boldsymbol{\theta}$ is the output vector. We use (1)–(4) to obtain the state-space model

$$\dot{\mathbf{x}} = \mathbf{f}(\mathbf{x}) + \mathbf{b}v \tag{5}$$

where

$$\mathbf{f}(\mathbf{x}) = \begin{bmatrix} \mathbf{x}_2 \\ \mathbf{D}^{-1}(\mathbf{x}_1)(-\mathbf{g}(\mathbf{x}_1) - \mathbf{K}\mathbf{x}_1 - \mathbf{C}(\mathbf{x}_1, \mathbf{x}_2)\mathbf{x}_2 + \mathbf{K}\mathbf{r}\mathbf{x}_3) \\ \mathbf{x}_4 \\ \mathbf{J}^{-1}(\mathbf{r}\mathbf{K}\mathbf{x}_1 - \mathbf{r}^2\mathbf{K}\mathbf{x}_3 - \mathbf{B}\mathbf{x}_4 + \mathbf{K}_m\mathbf{x}_5) \\ -\mathbf{L}^{-1}(\mathbf{K}_b\mathbf{x}_4 + \mathbf{R}\mathbf{x}_5) \end{bmatrix},$$

$$\mathbf{b} = \begin{bmatrix} \mathbf{0} \\ \mathbf{0} \\ \mathbf{0} \\ \mathbf{0} \\ \mathbf{L}^{-1} \end{bmatrix}, \qquad \mathbf{x} = \begin{bmatrix} \boldsymbol{\theta} \\ \dot{\boldsymbol{\theta}} \\ \boldsymbol{\theta}_m \\ \dot{\boldsymbol{\theta}}_m \\ \mathbf{I}_a \end{bmatrix}$$

The state-space model of the robotic system expressed by (5) shows a highly nonlinear coupled large system.

3 Robust control

To control such a complicated system, a control approach is proposed based on the voltage control strategy. The proposed controller design includes two interior loops; the inner loop controls the rotor position while the outer loop provides a desired rotor position for controlling the joint angle. Electrical equation of motor is given by

$$v = RI_a + L\dot{I}_a + k_b\dot{\theta}_m + \varphi(t) \tag{6}$$

where $\varphi(t)$ represents an external disturbance. It is very interesting to note that (6) is a single-input/single-output (SISO) system while the robot manipulator is a multivariable multi-input system. The motor current I_a contains effects of coupling between the motor and the manipulator. Thus, canceling this coupling will obtain a control law that is free of manipulator dynamics. We may write (6) by the use of nominal parameters as

$$v = \hat{R}I_a + \hat{k}_b\dot{\theta}_m + v_d \tag{7}$$

where $\hat{R}$ and $\hat{k}_b$ are the nominal parameters for the actual parameters given by R and k_b, respectively. The lumped uncertainty v_d may cover the parametric errors, unmodeled dynamics, and external disturbances. Substituting (6) into (7) yields

$$v_d = (R - \hat{R})I_a + L\dot{I}_a + (k_b - \hat{k}_b)\dot{\theta}_m + \varphi(t) \tag{8}$$

where v_d is the lumped uncertainty, $(R - \hat{R})I_a + (k_b - \hat{k}_b)\dot{\theta}_m$ expresses the effect of parametric uncertainty, $L\dot{I}_a$ represents the unmodeled dynamics and $\varphi(t)$ denotes the external disturbance. The lumped uncertainty v_d purposefully includes $L\dot{I}_a$ in (8). As a result, the obtained nominal model is free of $\dot{I}_a$ for control purposes. In practice, measurement of $\dot{I}_a$ is not common, however, it can be measured based on a principal that the induced voltage in a coil is proportional with $\dot{I}_a$.

The nominal parameters are known with our best knowledge about the actual parameters whereas the lumped uncertainty is unknown. To estimate the lumped uncertainty, we propose

$$\hat{v}_d(t) = v(t-\varepsilon) - \hat{R}I_a(t) - \hat{k}_b\dot{\theta}_m(t) \tag{9}$$

where $\hat{v}_d$ is the estimate of the lumped uncertainty and ε is a small positive value. We have used this kind of observer to estimate the uncertainty in the robust impedance control of a hydraulic suspension system [27]. A control law is proposed based on the feedback linearization as

$$v = \hat{R}I_a + \hat{k}_b u + \hat{v}_d(t) \tag{10}$$

where u is a new control input. $\hat{v}_d(t)$ is obtained using the available information stated by (9). Then, $\hat{v}_d(t)$ is used in the control command $v(t)$ given by (10). This means that $v(t)$ is not available when calculating $\hat{v}_d(t)$. Instead of $v(t)$, we have to use $v(t-\varepsilon)$ in the RHS of (9) to obtain $\hat{v}_d(t)$. The value of $v(t-\varepsilon)$ is a recent past information of $v(t)$. Substituting (9) into (10) yields

$$v = v(t-\varepsilon) + \hat{k}_b(u - \dot{\theta}_m) \tag{11}$$

A control law is proposed to track a desired trajectory as

$$u = \dot{\theta}_{md} + \beta(\theta_{md} - \theta_m) \tag{12}$$

where β is a constant gain and θ_{md} is the desired rotor angle provided by the outer loop.

Substituting (12) into (11) yields

$$v = v(t-\varepsilon) + \hat{k}_b\big(\dot{\theta}_{md} - \dot{\theta}_m + \beta(\theta_{md} - \theta_m)\big) \tag{13}$$

Assume that voltage of every motor is limited to protect the motor against over voltages. Therefore, control law (13) is modified as

$$v(t) = U \quad \text{for } |U| \le u_{\max} \tag{14}$$

$$v(t) = u_{\max}\operatorname{sgn}(U) \quad \text{for } u_{\max} < |U| \tag{15}$$

where $u_{\max}$ is a positive constant called as the maximum permitted voltage of motor and U is expressed as

$$U = v(t-\varepsilon) + \hat{k}_b\big(\dot{\theta}_{md} - \dot{\theta}_m + \beta(\theta_{md} - \theta_m)\big) \tag{16}$$

To track the desired joint angle, the outer loop is formed by a PID controller of the form

$$\theta_{md} = k_d\dot{e} + k_p e + k_i\int e\,dt \tag{17}$$

$$e = \theta_d - \theta \tag{18}$$

where k_p, k_d and k_i are proportional, derivative and integral gains, respectively. θ is the actual joint angle, θ_d is the desired joint angle, and e is the joint tracking error. The time derivative of PID controller in (17) is

$$k_d\ddot{e} + k_p\dot{e} + k_i e = \dot{\theta}_{md} \tag{19}$$

Substituting (19) into (16) yields

$$U = v(t-\varepsilon) + \hat{k}_b\big(k_d\ddot{e} + k_p\dot{e} + k_i e - \dot{\theta}_m + \beta(\theta_{md} - \theta_m)\big) \tag{20}$$

It is important to note that the proposed control law (14)–(17) is free of the manipulator dynamics and depends only on one parameter of motor denoted by $\hat{k}_b$. The obtained control law is similar to the time delay control from a point of view that employs the available information of the system response and the control inputs in the present and the recent past through the time delay. However, the proposed approach differs from the time delay control that calculates the estimate of uncertainty to obtain the control law. The estimate of uncertainty is not calculated to obtain the control law (14)–(17). Then, we use the voltage control strategy to develop a new control approach that requires only a few measurements rather than many measurements/estimations as used in the time delay control.

The position and velocity of the joint should be measured to form the PID controller in (17). In the case of using only the joint position measurement, the PID controller amplifies the measurement noise of the joint position through differentiation. The performance of the controller is then degraded in the face of the measurement noise. How to compensate the noise effects is an interesting topic that requires an extensive discussion.

4 Stability analysis and performance evaluation

Stability analysis of the control system is presented to evaluate the proposed control law in (14)–(17). Since the proposed control law is a decentralized control, stability analysis is presented for every individual joint to verify stability of the robotic system.

It follows from (7) that the lumped uncertainty v_d enters the system the same channel as the control input v. Thus, the uncertainty is said to satisfy the matching condition [28] or equivalently is said to be matched. This property ensures robust stabilizability [20].

To make the dynamics of the tracking error well defined such that the robot can track the desired trajectory, we make the following assumption.

Assumption 1 The desired trajectory θ_d must be smooth in the sense that θ_d and its derivatives up to a necessary order are available and all uniformly bounded.

As a necessary condition to design a robust control, the external disturbance must be bounded.

Assumption 2 The external disturbance $\varphi(t)$ is bounded as

$$|\varphi(t)| \leq \varphi_{\max} \tag{21}$$

where $\varphi_{\max}$ is a positive constant.

By multiplying both sides of (6) by I_a, one obtains the following power equation

$$vI_a = RI_a^2 + L\dot{I}_a I_a + k_b\dot{\theta}_m I_a + \varphi(t)I_a \tag{22}$$

Motor receives the electrical power expressed by vI_a to provide the mechanical power stated as $k_b\dot{\theta}_m I_a$ in (22). The power RI_a^2 is the loss in the windings and the power $L\dot{I}_a I_a$ is the time derivative of the magnetic energy. From (22), we can write for $t \geq 0$

$$\int_0^t \big(v - \varphi(t)\big) I_a \, dt = \int_0^t RI_a^2 \, dt + \int_0^t L\dot{I}_a I_a \, dt + \int_0^t k_b\dot{\theta}_m I_a \, dt \tag{23}$$

with $I_a(0) = 0$, (23) is

$$\int_0^t \big(v - \varphi(t)\big) I_a \, dt = RI_a^2 t + 0.5LI_a^2 + \int_0^t k_b\dot{\theta}_m I_a \, dt \tag{24}$$

Since $RI_a^2 t \geq 0$ and $0.5LI_a^2 \geq 0$,

$$\int_0^t k_b\dot{\theta}_m I_a \, dt \leq \int_0^t \big(v - \varphi(t)\big) I_a \, dt \tag{25}$$

The upper bound of mechanical energy is given by

$$\int_0^t k_b\dot{\theta}_m I_a \, dt = \int_0^t \big(v - \varphi(t)\big) I_a \, dt \tag{26}$$

Hence, at the upper bound of mechanical energy

$$k_b\dot{\theta}_{\mathrm{m}} = v - \varphi(t) \tag{27}$$

Therefore, $\dot{\theta}_{\mathrm{m}}$ is limited as

$$|\dot{\theta}_{\mathrm{m}}| \leq \big(|v| + |\varphi(t)|\big)/k_b \tag{28}$$

Control law (14)–(17) leads to

$$|v| \leq u_{\max} \tag{29}$$

Substituting (29) and (21) into (28) yields

$$|\dot{\theta}_{\mathrm{m}}| \leq (u_{\max} + \varphi_{\max})/k_b \triangleq \dot{\theta}_{m,\max} \tag{30}$$

where $\dot{\theta}_{m,\max}$ is the maximum velocity of motor.

From (6), we can write

$$RI_a + L\dot{I}_a = w \tag{31}$$

where

$$w = v - k_b\dot{\theta}_m - \varphi(t) \tag{32}$$

v, $\dot{\theta}_m$ and $\varphi(t)$ are bounded as stated by (29), (30) and (21), respectively. Consequently, the input w in (31) is bounded. The linear differential equation (31) is a stable linear system based on the Routh–Hurwitz criterion. Since the input w is bounded, the output I_a is bounded. From (31)

$$L\dot{I}_a = w - RI_a \tag{33}$$

Since w and I_a are bounded, $\dot{I}_a$ is bounded.

Control law (14)–(17) operate in two areas of $u_{\max} \leq |U|$ and $u_{\max} > |U|$. The tracking performance should be evaluated in both areas.

(a) *Area of* $|U| \le u_{\max}$ Substituting (14) into (6), one obtains the closed-loop system

$$v(t-\varepsilon) + \hat{k}_b\big(\dot{\theta}_{md} - \dot{\theta}_m + \beta(\theta_{md} - \theta_m)\big) = RI_a + L\dot{I}_a + k_b\dot{\theta}_m + \varphi(t) \tag{34}$$

From (6), we can write

$$v(t-\varepsilon) = RI_a(t-\varepsilon) + L\dot{I}_a(t-\varepsilon) + k_b\dot{\theta}_m(t-\varepsilon) + \varphi(t-\varepsilon) \tag{35}$$

Substituting (35) into (34) yields the closed-loop system

$$\dot{E} + \beta E = \eta(t) \tag{36}$$

where

$$E = \theta_{md} - \theta_m \tag{37}$$

represents the motor tracking error and $\eta(t)$ is expressed as

$$\eta(t) = \frac{R(I_a(t) - I_a(t-\varepsilon)) + L(\dot{I}_a(t) - \dot{I}_a(t-\varepsilon)) + k_b(\dot{\theta}_m(t) - \dot{\theta}_m(t-\varepsilon)) + \varphi(t) - \varphi(t-\varepsilon)}{\hat{k}_b} \tag{38}$$

where $\eta(t)$ is called the residual uncertainty in the closed-loop system. Since the variables $I_a(t)$, $\dot{I}_a(t)$, $\dot{\theta}_m(t)$, and $\varphi(t)$ are bounded, and $\hat{k}_b$ is a constant, then $\eta(t)$ is bounded as

$$|\eta(t)| \le \rho(t) \tag{39}$$

where $\rho(t)$ is a positive scalar called as the uncertainty bound parameter.

The residual uncertainty $\eta(t)$ can be expressed in terms of control efforts using (6) into (38) as

$$\eta(t) = \big(v(t) - v(t-\varepsilon)\big)/\hat{k}_b \tag{40}$$

From (40) and (29), one obtains that

$$|\eta(t)| \le \big(|v(t)| + |v(t-\varepsilon)|\big)/\hat{k}_b \le 2u_{\max}/\hat{k}_b \tag{41}$$

Solution of differential equation (36) is given by

$$E(t) = \exp(-\beta t)E(0) + \int_0^t \exp\big(-\beta(t-\tau)\big)\eta(\tau)\,d\tau \quad \text{for } t \ge 0 \tag{42}$$

where $E(0)$ is the initial motor tracking error. Since $\beta > 0$ and the residual uncertainty $\eta(t)$ is bounded, the motor tracking error $E(t)$ is bounded as

$$\begin{aligned} |E(t)| &\le |\exp(-\beta t)E(0)| + |\eta(t)|\left|\int_0^t \exp\big(-\beta(t-\tau)\big)\,d\tau\right| \\ &\le |\exp(-\beta t)E(0)| + |\eta(t)|/\beta \end{aligned} \tag{43}$$

Since $\exp(-\beta t) \to 0$ as $t \to \infty$, $|E(t)| \to |\eta(t)|/\beta$ as $t \to \infty$. If the initial error be zero, $|E(t)| \le |\eta(t)|/\beta$.

Evaluation of the tracking performance presented by (42) and (43) is twofold.

(1) The motor tracking error converges exponentially with a time constant of $1/\beta$.
(2) The tracking error is within the precision of $|\eta(t)|/\beta$ for $t \ge 0$ if $E(0) \simeq 0$, otherwise, this precision is obtained after about $t \ge 5/\beta$.

If the uncertainty bound parameter ρ is sufficiently small, the motor tracking error E in (36) stays close to zero for an initial error $E(0) \simeq 0$. In the case of $E(0) = 0$, the tracking error is bounded from (43) as

$$|E(t)| \le |\eta(t)|/\beta \le \rho/\beta \quad \text{for } t \ge 0 \tag{44}$$

In order to consider boundedness of the joint tracking error e, substituting (19) and (37) into (36) yields the dynamics of closed-loop system as

$$k_d\ddot{e} + k_p\dot{e} + k_i e = \eta(t) + \dot{\theta}_m - \beta E \tag{45}$$

All three terms $\eta(t)$, $\dot{\theta}_m$ and E in the RHS of (45) are bounded as stated by (39), (30) and (43), respectively. System (45) is a second order linear system with a bounded input given by $\eta(t) + \dot{\theta}_m - \beta E$. Since the input is bounded and all three gains k_d, k_p and k_i are positive, system (45) is stable based on the Routh–Hurwitz criteria. Therefore, e, $\dot{e}$ and $\ddot{e}$ are bounded.

Since the desired joint angle θ_d and its time derivative $\dot{\theta}_d$ are bounded, the bounded variables e and $\dot{e}$ imply that $\theta = \theta_d - e$ and $\dot{\theta} = \dot{\theta}_d - \dot{e}$ are bounded. Since

I_a is limited, (4) implies that τ is bounded. From (2), we have

$$J\ddot{\theta}_m + B\dot{\theta}_m + r^2 K\theta_m = \tau + rK\theta \tag{46}$$

System (57) is a second order linear system with positive gains J, B, r^2K, and a limited input $\tau + rK\theta$. This system is stable based on the Routh-Hurwitz criterion and implies that θ_m, $\dot{\theta}_m$ and $\ddot{\theta}_m$ are bounded. Since all states associated with each joint i.e. θ, $\dot{\theta}$, θ_m, $\dot{\theta}_m$, and I_a are bounded, vectors $\boldsymbol{\theta}$, $\dot{\boldsymbol{\theta}}$, $\boldsymbol{\theta}_m$, $\dot{\boldsymbol{\theta}}_m$, and $\mathbf{I}_a$ are bounded. As a result, the robotic system in (5) has the Bounded-Input/Bounded-Output (BIBO) stability.

(b) *Area of* $u_{\max} < |U|$ To consider the convergence of tracking error E in the area that $u_{\max} \le |U|$, a positive definite function is proposed as

$$V = 0.5k_b E^2 \tag{47}$$

where $V(0) = 0$ and $V(E) > 0$ for $E \neq 0$. The time derivative of $V$is calculated as

$$\dot{V} = k_b E\dot{E} \tag{48}$$

Substituting control law (15) into (6) forms the closed-loop system

$$RI_a + L\dot{I}_a + k_b\dot{\theta}_m + \varphi(t) = u_{\max}\mathrm{sgn}(U) \tag{49}$$

Substituting (37) and (49) into (48) yields

$$\begin{aligned}\dot{V} &= E(k_b\dot{\theta}_{md} - k_b\dot{\theta}_m)\\ &= E\big(k_b\dot{\theta}_{md} + RI_a + L\dot{I}_a + \varphi(t) - u_{\max}\mathrm{sgn}(U)\big)\end{aligned} \tag{50}$$

Assume that there exits a positive scalar denoted by μ that

$$\big|k_b\dot{\theta}_{md} + RI_a + L\dot{I}_a + \varphi(t)\big| < \mu \tag{51}$$

To establish the convergence, the condition $\dot{V} < 0$ should be satisfied. For this purpose, it is sufficient that

$$u_{\max}\mathrm{sgn}(U) = \mu\mathrm{sgn}(E) \tag{52}$$

Proof Substituting (52) into (50) yields

$$\dot{V} = E\big(k_b\dot{\theta}_{md} + RI_a + L\dot{I}_a + \varphi(t) - \mu\mathrm{sgn}(E)\big) \tag{53}$$

Since

$$\begin{aligned}&E\big(k_b\dot{\theta}_{md} + RI_a + L\dot{I}_a + \varphi(t)\big)\\ &\quad\le |E|\big|k_b\dot{\theta}_{md} + RI_a + L\dot{I}_a + \varphi(t)\big| < |E|\mu\end{aligned} \tag{54}$$

Hence

$$E\big(k_b\dot{\theta}_{md} + RI_a + L\dot{I}_a + \varphi(t)\big) - \mu|E| < 0 \tag{55}$$

Using $E\,\mathrm{sgn}(E) = |E|$ into (54) yields

$$\dot{V} = E\big(k_b\dot{\theta}_{md} + RI_a + L\dot{I}_a + \varphi(t)\big) - \mu|E| \tag{56}$$

Substituting (55) into (56) proves that $\dot{V} < 0$. Thus, the motor tracking error is converged until the control system comes into the area governed by control law (14). As discussed above, even if the robotic system starts from the area of $u_{\max} < |U|$, it goes into the area of $|U| \le u_{\max}$. Equation (52) implies that

$$u_{\max} = \mu \tag{57}$$

Therefore, the maximum voltage of motor should satisfy (57) for the convergence of the tracking error E.

As mentioned above, starting from an arbitrary $E(0)$ under the condition $u_{\max} = \mu$, value of $|E|$ is reduced and motor will move to the area of $u_{\max} \ge |U|$ that all states are bounded. From the closed-loop system (49), we can obtain

$$RI_a + L\dot{I}_a = u_{\max}\mathrm{sgn}(U) - k_b\dot{\theta}_m - \varphi(t) \tag{58}$$

The RHS of (58) is bounded as

$$\begin{aligned}&\big|u_{\max}\mathrm{sgn}(U) - k_b\dot{\theta}_m\big|\\ &\quad\le |u_{\max}|\big|\mathrm{sgn}(U)\big| + |k_b\dot{\theta}_m| + \big|\varphi(t)\big|\\ &\quad\le u_{\max} + k_b\dot{\theta}_{m,\max} + \varphi_{\max}\end{aligned} \tag{59}$$

Thus, the linear stable system (58) under the bounded input $u_{\max}\mathrm{sgn}(U) - k_b\dot{\theta}_m - \varphi(t)$ obtains the bounded output I_a. Since I_a is limited, (4) implies that τ is bounded. Then, linear stable system (46) under bounded input $\tau + rK\theta$ obtains that variable $\theta_m, \dot{\theta}_m$ and $\ddot{\theta}_m$ are bounded. Consider (19) as a second order linear system with positive gains and a limited input $\dot{\theta}_{md}$. Thus e, $\dot{e}$ and $\ddot{e}$ are bounded. Since the desired joint angle θ_d and its time derivative $\dot{\theta}_d$ are bounded, the bounded variables e, and $\dot{e}$ imply that $\theta = \theta_d - e$ and $\dot{\theta} = \dot{\theta}_d - \dot{e}$ are bounded. Since all states θ, $\dot{\theta}$, θ_m, $\dot{\theta}_m$, and I_a associated with each joint are bounded then vectors $\boldsymbol{\theta}$, $\dot{\boldsymbol{\theta}}$, $\boldsymbol{\theta}_m$, $\dot{\boldsymbol{\theta}}_m$, and $\mathbf{I}_a$ are bounded. As a conclusion of this analysis, the robotic system in (5) has the BIBO stability. □

5 Uncertainty estimation

It is worthy to note that the lumped uncertainty stated in (8) includes the parametric uncertainty, unmodeled dynamics and external disturbances. The lumped uncertainty, v_d, is unknown and enters to the system as an unwanted input, however, can be compensated by a suitable controller. We wish to know whether the estimate of the lumped uncertainty converges to its actual value or not. From (7) and (9) we have

$$v_d - \hat{v}_d = v(t) - v(t-\varepsilon) \tag{60}$$

As a result, the estimation error expressed as $v_d - \hat{v}_d$ is given by the change of control input in the period of ε stated as $v(t) - v(t-\varepsilon)$ in (60). If $\dot{v}(t) - \dot{v}(t-\varepsilon)$ is bounded, value of $v(t) - v(t-\varepsilon)$ will be small in a given small value to ε. This means that $v(t) \simeq v(t-\varepsilon)$ if ε is selected close to zero. The time delay ε as a control design parameter has a main role in the performance of uncertainty estimation.

Control law (14)–(17) verifies that $v(t) = u_{\max}$ if $U > u_{\max}$, $v(t) = -u_{\max}$ if $U < -u_{\max}$, and $v(t) = U$ if $|U| \leq u_{\max}$. Consequently, it can be said that $v(t)$ is a saturation function denoted as $v(t) = sat(U)$ with the upper limit $u_{\max}$ and the lower limit $-u_{\max}$. We can conclude that $v(t)$ is a continuous function of U. When robotic system operates in the areas $U > u_{\max}$ or $U < -u_{\max}$, control law $v(t)$ is constant, implying $v(t) = v(t-\varepsilon)$, thus $v_d = \hat{v}_d$. Therefore, estimation error is zero. We are concerned about the area of $|U| \leq u_{\max}$. Taking the time derivatives of (36) and using (40) one obtains

$$\ddot{E} + \beta \dot{E} = \big(\dot{v}(t) - \dot{v}(t-\varepsilon)\big)/\hat{k}_b \tag{61}$$

As verified in Sect. 4, $\ddot{\theta}_m$, $\dot{\theta}_m$ and θ_m are bounded. In addition, the desired trajectory θ_{md} and its time derivatives $\dot{\theta}_{md}$ and $\ddot{\theta}_{md}$ are the bounded signals. Thus, $\ddot{E} = \ddot{\theta}_{md} - \ddot{\theta}_m$ and $\dot{E} = \dot{\theta}_{md} - \dot{\theta}_m$ are bounded. Therefore, $(\dot{v}(t) - \dot{v}(t-\varepsilon))/\hat{k}_b$ expressed in (61) is necessarily bounded. As a result, $v(t) \simeq v(t-\varepsilon)$ if the time delay ε is selected close to zero. Consequently, the lumped uncertainty is estimated well using the proposed novel estimation method.

6 Simulation

The proposed control law is applied to control an articulated robot manipulator with a symbolic representation in Fig. 1. The Denavit-Hartenberg (DH) parameters of the articulated robot are given in Table 1, where the parameters θ_i, d_i, a_i and α_i are called the joint angle, link offset, link length and link twist, respectively. Parameters of the manipulator are given in Table 2, where for the ith link, m_i is the mass, $r_{ci} = [x_{ci}\ y_{ci}\ z_{ci}]^T$ is the center of mass of the ith

Table 1 The Denavit–Hartenberg parameters

Link	θ	d	a	α
1	θ_1	d_1	0	$\pi/2$
2	θ_2	0	a_2	0
3	θ_3	0	a_3	0

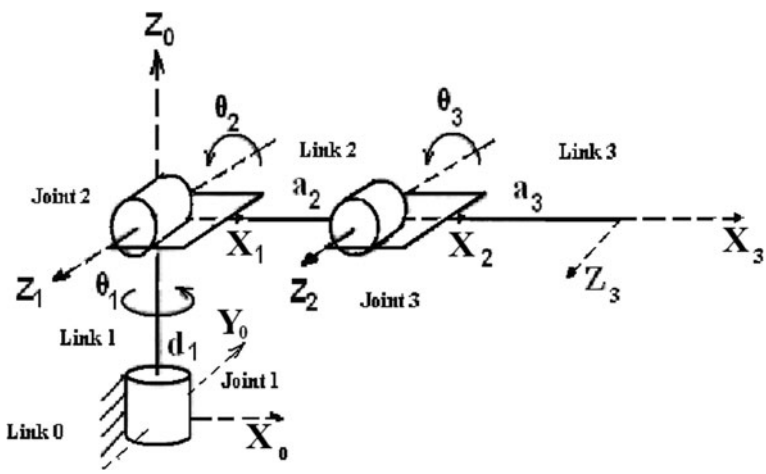

Fig. 1 Symbolic representation of the articulated robot

Table 2 The dynamical parameters

Link	DH	x_i	y_i	z_i	m_i	I_{xxi}	I_{yyi}	I_{zzi}	I_{xyi}	I_{xzi}	I_{yzi}
1	$d_1 = 0.280$	0	−0.22	0	19	0.34	0.36	0.31	0	0	0
2	$a_2 = 0.760$	−0.51	0	0	18.18	0.18	1.32	1.31	0	0	0
3	$a_3 = 0.930$	−0.67	0	0	10.99	0.07	0.92	0.93	0	0	0

Table 3 The motor parameters

Motors	v	R	K_b	L	J	B	r	k
1, 2, 3	40	1.6	0.26	0.001	0.0002	0.001	0.02	500

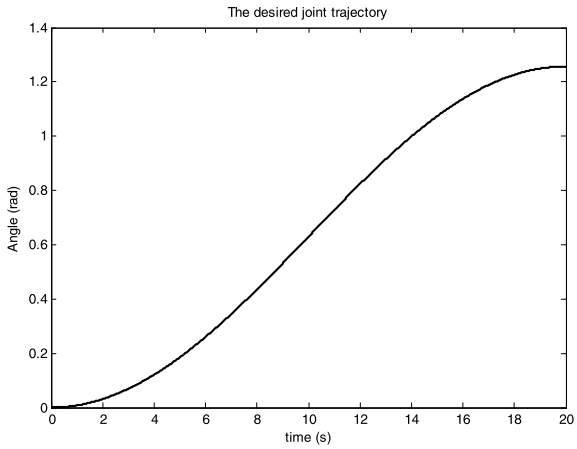

Fig. 2 The desired joint trajectory

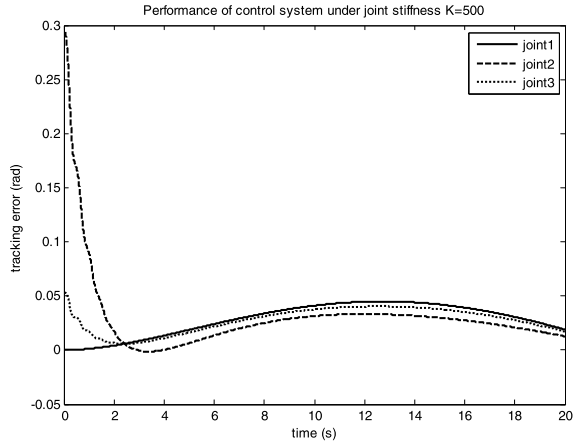

Fig. 3 Performance of control system under joint stiffness $k = 500$

frame. The inertia tensor in the center of mass frame is expressed as

$$I_i = \begin{bmatrix} I_{xxi} & I_{xyi} & I_{xzi} \\ I_{xyi} & I_{yyi} & I_{yzi} \\ I_{xzi} & I_{yzi} & I_{zzi} \end{bmatrix} \tag{62}$$

Motor parameters are given in Table 3. The control law depends only on one parameter of motor given by $\hat{k}_b$ as the nominal value of k_b. To consider the parametric uncertainties, $\hat{k}_b$ is assumed to be 95% of the real value k_b. The external disturbance is assumed as a pulse function to consider a sudden change with a period of 10 sec and amplitude of 1 V inserted to the voltage input of each motor. This is just an example of any bounded disturbances. The maximum voltage of each is set to $u_{\max} = 50$ V. The desired joint trajectory for the joints is shown in Fig. 2. The desired trajectory should be sufficiently smooth such that all its derivatives up to the required order are bounded. The control laws for all three motors are the same with the gain values of $\beta = 1$, $\varepsilon = 0.001$ s, $k_p = 500$, $k_d = 12$ and $k_i = 200$ selected by trial and error method to show a satisfactory performance. An optimization algorithm such as particle swarm optimization algorithm can be applied to find an optimum values for control design parameters to achieve a desired performance [29].

Simulation 1 Performance of the control system is shown in Fig. 3 while the joint tracking error reduces. The initial tracking errors are high since the joint stiffness is low and the manipulator is under a high load when starting. The least initial tracking error occurs in joint 1 and the highest one occurs in joint 3. The motors behave well under the permitted voltages as shown in Fig. 4. The motor voltages oscillate when starting to compensate the errors caused by the load torque. In addition, it has a fast response to compensate the external disturbance as presented by sudden changes on the curves. The control efforts are under the permitted voltages without chattering problem.

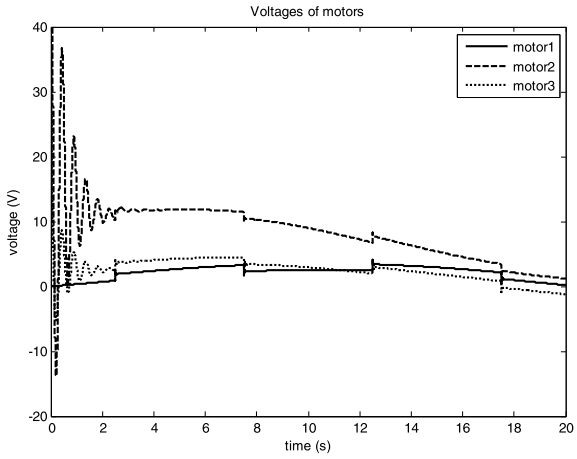

Fig. 4 Voltages of motors

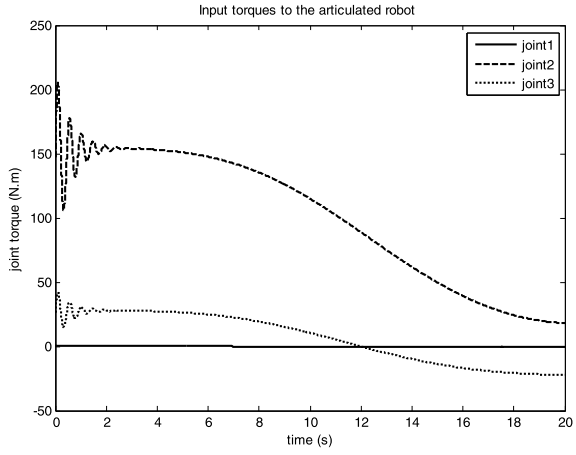

Fig. 5 Joint torques of the articulated robot

The joint torques are shown in Fig. 5. Joint 1 has the least torque while Joint 2 has the highest torque. Since the joints experience different loads, the control efforts behave differently to compensate for the errors.

Simulation 2 The time delay ε has a significant role in the performance of controller to overcome uncertainties. A smaller ε provides a smaller estimation error $v_d - \hat{v}_d$. A comparison on the performance of controller in different values of the time delay is shown in Fig. 6. As the time delay decreases the tracking error decreases. However, the same results are provided for the time delay $\varepsilon = 0.001$ s and $\varepsilon = 0.0005$ s. This may be due to some limitations in the computation algorithm use for simulation.

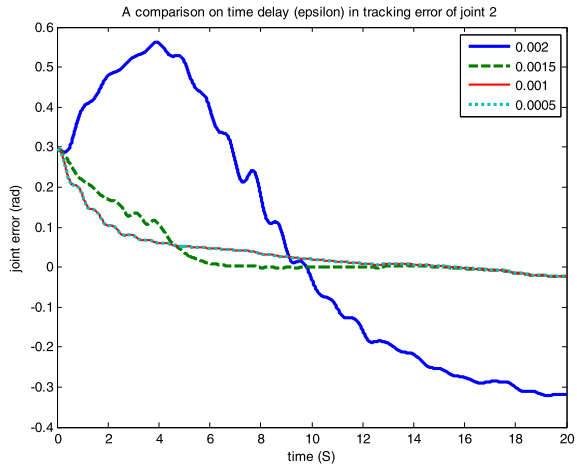

Fig. 6 A comparison on time delay ε in tracking error of joint 2

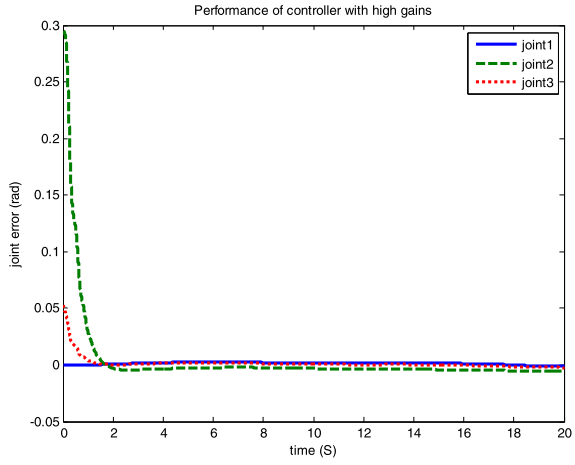

Fig. 7 Performance of controller with high gains

Simulation 3 The control law is checked for different gains. The control system is stable and the tracking error is bounded. As the gains k_p, k_d and k_i are increased, the tracking error is decreased. However, the sensitivity of control system becomes higher. Performance of the control law with the high gains $k_p = 4000, k_d = 100$ and $k_i = 10000$ is shown in Fig. 7. We set $\beta = 0.1$ and $\varepsilon = 0.001$ s in this simulation. The tracking error has been highly reduced in compared with Fig. 3. The control efforts are still satisfactory as shown in Fig. 8.

Simulation 4 This simulation is for considering a large parametric uncertainty. The tracking perfor-

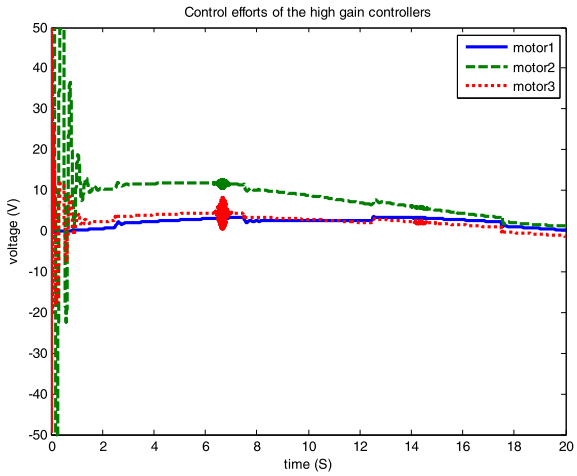

Fig. 8 Control efforts high-gain controllers

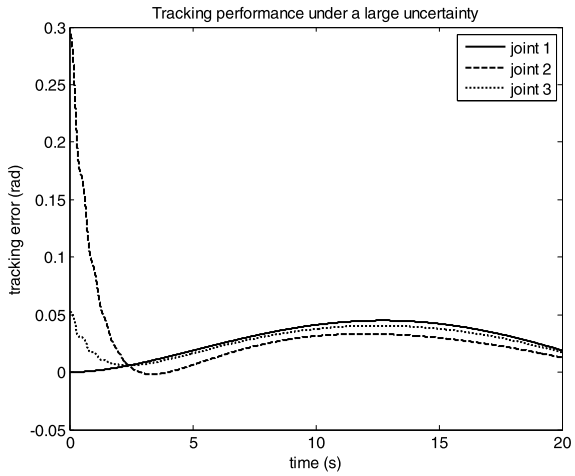

Fig. 9 Tracking performance under $\hat{k}_b = 0.8k_b$

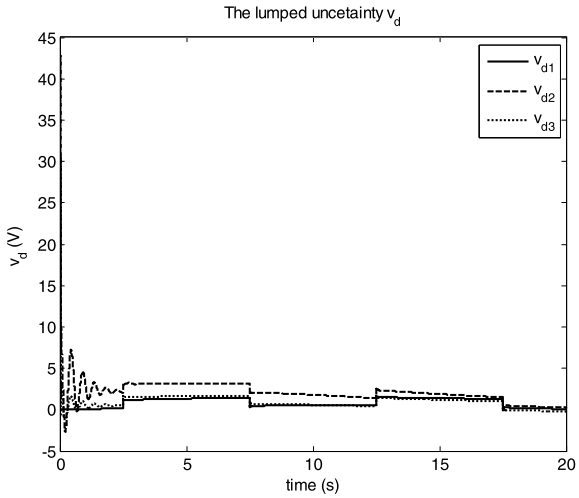

Fig. 10 Lumped uncertainty

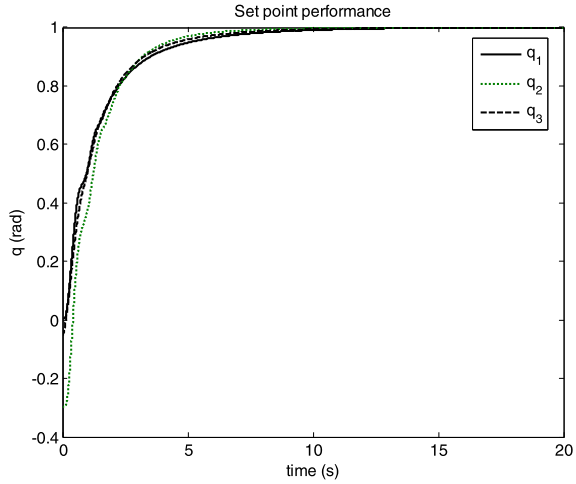

Fig. 11 Set point performance

mance is presented for a given $\hat{k}_b = 0.8k_b$ while other control design parameters are the same as Simulation 1. The performance of control system is shown in Fig. 9. It behaves roughly the same as case $\hat{k}_b = 0.95k_b$ shown in Fig. 3. The lumped uncertainty v_d is bounded as shown in Fig. 10. It jumps initially because of the effect of $\dot{I}_a$ and presents a pulse function due to the given external disturbances.

Simulation 5 Set point control is simulated. The external disturbance is removed, however, the parametric uncertainty is given by $\hat{k}_b = 0.8k_b$. The desired joint angles are set to 1 rad. The control law for three motors is the same with the gains $\beta = 1$, $\varepsilon = 0.001$ s, $k_p = 100$, $k_d = 10$ and $k_i = 65$. Set point performance is shown in Fig. 11. The joint tracking error asymptotically approaches zero as expected.

Simulation 6 Performance of the controller is evaluated in tracking a fast varying trajectory. The motor velocity is limited as stated in (30). Therefore, we should check whether velocity of the desired fast varying trajectory is permitted or not. If velocity of the desired trajectory becomes twice as one used in Simulation 1, it is still permitted. In this case, the control efforts perform well, however, the joint tracking errors will be higher than ones in Simulation 1. After

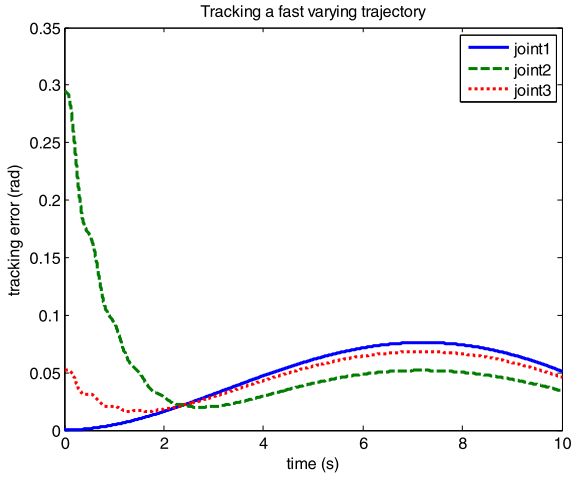

Fig. 12 Tracking a fast varying trajectory

starting, the maximum value of the tracking error for joint 1 reaches to about 0.077 rad in Fig. 12 while it is about 0.045 rad in Fig. 3 for Simulation 1. The PID gains can be regulated to decrease the tracking error.

Simulations have presented tracking performance through figures. They present the following results.

(a) All presented signals are bounded.
(b) Joint tracking error presents a limited precision in the tracking application, and approaches zero in the set point application.
(d) Control efforts behave well within their limits without chattering problem.
(e) Selecting a smaller time delay presents a smaller tracking error.

7 Conclusion

The voltage control strategy is superior to the torque-control strategy in the control of electrically driven robot manipulators. The torque-control laws are involved in the complexity of manipulator dynamics whereas the voltage control is free of manipulator dynamics. The proposed control law has performed well on a flexible-joint robot that has a complicated dynamics. It has been proven that the closed-loop system has the BIBO stability. Simulation results present a good tracking performance of the control system as verified by performance evaluation. The tracking error approaches zero in the set point application and converges to a limited precision in the tracking application. Among the control design parameters, the time delay ε has a main role in the performance of uncertainty estimation. A smaller time delay provides a smaller estimation error and a smaller tracking error, as well.

References

1. Sweet, L.M., Good, M.C.: Redefinition of the robot motion control problem. IEEE Control Syst. Mag. **5**(3), 18–24 (1985)
2. Brogliato, B., Ortega, R., Lozano, R.: Global tracking controllers for flexible-joint manipulators: a comparative study. Automatica **31**(7), 41–956 (1995)
3. Tomei, P.: A simple PD controller for robots with elastic joints. IEEE Trans. Autom. Control **36**(10), 1208–1213 (1991)
4. Luca, A.D., Isidori, A., Nicolo, F.: Control of robot arm with elastic joints via nonlinear dynamic feedback. In: The 24th Conf. Decision Contr., Ft. Lauderdale, FL, pp. 1671–1679 (1985)
5. Spong, M.W., Khorasani, K., Kokotovic, P.V.: An integral manifold approach to the feedback control of flexible joint robots. IEEE J. Robot. Autom. **RA-3**, 291–300 (1987)
6. Marino, R., Nicosia, S.: Singular perturbation techniques in the adaptive control of elastic robots. In: The IFAC Symp. Robot Contr., Barcelona, Spain (1985)
7. Spong, M.W.: Modeling and control of elastic joint robots. ASME J. Dyn. Syst. Meas. Control **109**, 310–319 (1987)
8. Wilson, G.A.: Robust tracking of elastic joint manipulators using sliding mode control. Trans. Inst. Meas. Control **16**(2), 99–107 (1994). doi:10.1177/014233129401600206
9. Spong, M.W.: Adaptive control of flexible joint manipulators: comments on two papers. Automatica **31**(4), 585–590 (1985)
10. Chang, L.L., Chuan, C.C.: Rigid model-based fuzzy control of flexible-joint manipulators. J. Intell. Robot. Syst. **13**(2), 107–126 (1995). doi:10.1007/BF01254847
11. Wang, D.: A simple iterative learning controller for manipulators with flexible joints. Automatica **31**(9), 1341–1344 (1995)
12. Zeman, V., Patel, R.V., Khorasani, K.: Control of a flexible-joint robot using neural networks. IEEE Trans. Control Syst. Technol. **5**(4), 453–462 (1997). doi:10.1109/87.595927
13. Kugi, A., Ott, C., Albu-Schaffer, A., Hirzinger, G.: On the passivity-based impedance control of flexible joint robots. IEEE Trans. Robot. Autom. **24**(2), 416–429 (2008). doi:10.1109/TRO.2008.915438
14. Talole, E., Kolhe, P., Phadke, B.: Extended state observer based control of flexible joint system with experimental validation. IEEE Trans. Ind. Electron. (2009). doi:10.1109/TIE.2009.2029528
15. Youcef-Toumi, K., Shortlidge, C.: Control of robot manipulators using time delay. In: IEEE Int. Conf. on Robotics and Automation, Sacramento, CA (1991)

16. Talole, S.E., Phadke, S.B.: Model following sliding mode control based on uncertainty and disturbance estimator. ASME J. Dyn. Syst. Meas. Control **130**, 1–5 (2008)
17. Marino, R., Nicosia, S.: Singular perturbation techniques in the adaptive control of elastic robots. Presented at the IFAC Symp. Robot Contr., Barcelona, Spain, 1985
18. Tomei, P.: An observer for flexible joint robots. IEEE Trans. Autom. Control **35**(6), 739–743 (1990). doi:10.1109/9.53558
19. De Luca, A., Lanari, L.: Robots with elastic joints are linearizable via dynamic feedback. In: 34th IEEE Conf. on Decision and Control, New Orleans, LA (1995)
20. Qu, Z., Dawson, D.M.: Robust Tracking Control of Robot Manipulators. IEEE Press, New York (1996)
21. Abdallah, C., Dawson, D., Dorato, P., Jamshidi, M.: Survey of robust control for rigid robots. IEEE Control Syst. Mag. **11**, 24–30 (1991)
22. Cheah, C.C., Hirano, M., Kawamura, S., Arimoto, S.: Approximate Jacobian control for robots with uncertain kinematics and dynamics. IEEE Trans. Robot. Autom. **19**(4), 692–702 (2003)
23. Fateh, M.M., Soltanpour, M.R.: Robust task-space control of robot manipulators under imperfect transformation of control space. Int. J. Innov. Comput. Inf. Control **5**(11A), 3949–3960 (2009)
24. Fateh, M.M.: Proper uncertainty bound parameter to robust control of electrical manipulators using nominal model. Nonlinear Dyn. **61**(4), 655–666 (2010). doi:10.1007/s11071-010-9677-7
25. Fateh, M.M.: On the voltage-based control of robot manipulators. Int. J. Control. Autom. Syst. **6**(5), 702–712 (2008)
26. Fateh, M.M.: Robust voltage control of electrical manipulators in task-space. Int. J. Innov. Comput. Inf. Control **6**(6), 2691–2700 (2010)
27. Fateh, M.M.: Robust impedance control of a hydraulic suspension system. Int. J. Robust Nonlinear Control **20**(8), 858–872 (2010). doi:10.1002/rnc.1473
28. Corless, M., Leitmann, G.: Continuous state feedback guaranteeing uniform ultimate boundedness for uncertain dynamics systems. IEEE Trans. Autom. Control **26**, 1139–1144 (1981)
29. Kennedy, J., Eberhart, R.: Particle swarm optimization. In: Proc. IEEE Int. Conf. Neural Networks, Perth, WA, Australia (1995)